Geophysical Research Letters

RESEARCH LETTER
10.1029/2021GL092652

Key Points:

- We present in situ observation of the guiding effect of whistler mode waves by the plasmapause with NASA's Van Allen Probes data
- The guiding effect is resulted from the combined effect of the inhomogeneous magnetic field and plasma density
- Whistler mode waves around the inner (outer) edge of plasmapause guided by high density duct-like (low density duct-like) density gradient, tend to have small (large) wave normal angles

Correspondence to:
X. Gao,
gaoxl@mail.ustc.edu.cn

Citation:
Chen, R., Gao, X., Lu, Q., Tsurutani, B. T., & Wang, S. (2021). Observational evidence for whistler mode waves guided/ducted by the inner and outer edges of the plasmapause. *Geophysical Research Letters*, *48*, e2021GL092652. https://doi.org/10.1029/2021GL092652

Received 25 JAN 2021
Accepted 14 FEB 2021

Observational Evidence for Whistler Mode Waves Guided/Ducted by the Inner and Outer Edges of the Plasmapause

Rui Chen[1,2], Xinliang Gao[1,2], Quanming Lu[1,2], Bruce T. Tsurutani[3], and Shui Wang[1,2]

[1]CAS Key Laboratory of Geospace Environment, School of Earth and Space Sciences, University of Science and Technology of China, Hefei, China, [2]CAS Center for Excellence in Comparative Planetology, Hefei, China, [3]Retired, Pasadena, CA, USA

Abstract We present observational support for whistler mode waves guidance by the plasmapause gradients based on a case study and statistical analyses. Due to the combined effects of inhomogeneous magnetic fields and plasma densities, whistler mode waves near the inner edge of plasmapause (plasmasphere side) will be guided by a high density duct-like (HDD) gradient, and tend to have very small wave normal angles (WNAs ≤ 20°) relative to the ambient magnetic field,B0. In contrast, whistler mode waves near the outer edge of the plasmapause (plasmatrough side) guided by a low density duct-like (LDD) gradient, tend to have quite large WNAs (≥∼60°). Statistical analyses emphasize these remarkably different properties of waves in the plasmapause gradients. The results indicate that the wave ducting effects at the plasmapause may lead to unusual and anomalous energetic pitch angle scattering.

Plain Language Summary The plasmapause is a naturally formed transition region with a sharp gradient in density, dividing the Earth's magnetosphere into two physically distinct plasma regions: a dense inner region (i.e., plasmasphere) and a tenuous outer region (i.e., plasma trough). Whistler mode waves guidance by the inner and outer edges of plasmapause have been predicted by ray tracing studies and electron magnetohydrodynamics simulations. However, to date no direct observational evidence has been reported due to the lack of simultaneous measurements of waves and detailed plasma densities with sufficiently high resolution and reliability. We use Van Allen Probes (RBSP) orbiting satellite data to present in situ observations of whistler wave guidance by plasmapause gradients. Our analyses reveal that whistler mode waves near the inner edge of plasmapause are guided by a high density duct (HDD)-like density gradient, and tend to have small wave normal angles (WNAs ≤ 20°). Whistler mode waves near the outer edge of the plasmapause are guided by a low density duct (LDD)-like density gradient, and tend to have large WNAs (≥∼60°). These results reveal that the plasmapause can guide whistler waves and lead to unusual and anomalous pitch angle scattering.

1. Introduction

Whistler mode waves such as chorus are one of the most intense electromagnetic emissions within the frequency range of 0.1–1.0 f_{ce} (f_{ce} is the equatorial electron gyrofrequency) in the Earth's magnetosphere (Burtis & Helliwell, 1969; Gao, Li, et al., 2014; Gao, Lu, et al., 2018; Tsurutani & Smith, 1974). It is well accepted that whistler mode waves can accelerate seed energetic electrons (∼100 keV) to relativistic energies ∼1 MeV (Horne et al., 2005; Thorne, Li, et al., 2013). The same waves can also scatter low-to medium energy (0.1–100 keV) electrons into the loss cone causing precipitation into the upper atmosphere (Ni et al., 2008; Thorne, Ni, et al., 2010; Tsurutani et al., 2013). The distribution and polarization properties (such as the direction of propagation relative to the ambient magnetic field, B0) of whistler mode waves are crucial toward understanding and modeling energetic electron dynamics in the geo-space environment (Artemyev, Agapitov, Breuillard, et al., 2012; Mourenas, Artemyev, Ripoll, et al., 2012; Ni et al., 2008), which are found to be significantly modulated by the background plasma density irregularities (i.e., low density duct [LDD] and high density duct [HDD], Koons, 1989; Li, Bortnik et al., 2011; Moullard et al., 2002; Smith et al., 1968). Both theoretical (Karpman & Kaufman, 1982; Scarabucci & Smith, 1971; Smith et al., 1960) and experimental studies (Streltsov & Bengtson, 2020; Streltsov et al., 2006; Woodroffe et al., 2013) have shown that whistler mode waves can be efficiently confined within density ducts and maintain their polarization properties dur-

ing propagation. Lower-band whistler mode waves with small wave normal angles (i.e., WNAs less than the Gendrin angle) can be guided by HDDs, and keep small WNAs during propagation. Whistler mode waves with large WNAs (i.e., larger than the Gendrin angle) can be guided by LDDs.

The plasmapause is the transition region between a dense plasma inner region (i.e., plasmasphere) and a tenuous, low beta outer region (i.e., outer magnetosphere) in the Earth's magnetosphere. The plasmapause is identified as the outermost sharp gradient in density (Carpenter, 1968; Carpenter & Anderson, 1992). Previous theories and ray-tracing analysis suggested that whistler mode waves could be effectively guided along the plasmapause's inner and outer edges (Inan & Bell, 1977) due to the combined effects of the inhomogeneous magnetic field and density gradients. The inner edge is equivalent to a HDD, where whistler mode waves with $f < 0.5f_{ce}$ and WNA smaller than the Gendrin angle will be trapped (Inan & Bell, 1977; Woodroffe & Streltsov, 2013). The outer edge functions as a LDD, where whistler mode waves with $f < 0.5f_{ce}$ and WNA larger than the Gendrin angle are expected to be guided by the outer edge (Inan & Bell, 1977; Woodroffe & Streltsov, 2013). Recently, based on equations of electron magnetohydrodynamics, Woodroffe and Streltsov (2013) have simulated the evolution of whistler mode waves near the two edges of the plasmapause. They obtained results which were consistent with theoretical predictions.

Because no observational evidence of this theory has been reported to date (Bryant et al., 1985; Cornilleau-Wehrlin et al., 1997; Li, Thorne, et al., 2010), it is the purpose of this paper to attempt to do so. In this study, we have presented the guiding effect of whistler waves by the plasmapause with NASA's Van Allen Probes data. A detailed case study on one plasmapause crossing clearly reveals different guiding effects of the inner and outer edges of plasmapause. Moreover, we have also conducted statistical analyses of whistler mode waves detected near the plasmapause, and confirmed their different properties around the inner and outer edges. Our results not only provide observational evidence for the guiding effect of whistler mode waves by the plasmapause gradients, but also shed light on the role of plasmapause in possibly modulating electron dynamics in the Earth's magnetosphere.

2. Data Sources

The Van Allen Probes (Mauk et al., 2013; previously named the Radiation Belt Storm Probes or RBSP), consists of twin satellites (A and B), operates entirely within the Earth's radiation belt and carries a number of instruments and instrument suites. In this study, we will use the Electric and Magnetic Field Instrument Suite and Integrated Science (EMFISIS, Kletzing et al., 2013) which provides low-resolution magnetic field data (64°S/sec), survey-mode wave power spectra (1/6 S/sec) from 10 Hz to 12 kHz, and high-frequency electric power spectra (1/6 S/sec). The low-resolution magnetic fields are treated as the background magnetic field. Detailed polarization information of whistler mode waves is also provided by the survey-mode spectral data. The background plasma densities are derived in two ways, both based on the upper hybrid wave band (Kurth et al., 2015) and also inferred from the spacecraft potential measured by the Electric Field and Waves instrument (EFW, Wygant et al., 2013). It is found that the densities derived by the two techniques were consistent with each other, giving confidence that the density values were accurate. All the data used in this study can be accessed from https://spdf.gsfc.nasa.gov/pub/data/rbsp/.

3. Case Study

This plasmapause crossing is recorded by RBSP-A during 06:00–06:50 UT on January 9, 2014. As the spacecraft moves radially away from the Earth from $L = 3.2$ to $L = 4.7$ there are also some slight changes in its MLT (10.2–11.7 h) and MLAT (−12.6° to −16.3°). In general, this small motion is not important for this study. Figure 1a shows the electron density obtained from the two different methods discussed in Section 2. The density inferred from the upper-hybrid wave frequency is indicated by the red line. The density estimated from the spacecraft potential is given by the black line. The two different estimates are quite similar, giving us confidence of the accuracy as mentioned previously. The plasmapause is first encountered at 06:20 UT. The electron density decreases rapidly until the probe enters the outer magnetosphere at 06:25 UT. The shaded region in Figure 1a marks the plasmapause. The magnetic power spectrum and WNA of whistler mode waves are given in Figures 1b and 1c, respectively. Whistler mode waves such as chorus are confined to the lower band (0.1–0.5f_{ce}, Tsurutani & Smith, 1974) and are distributed across the entire plasmapause

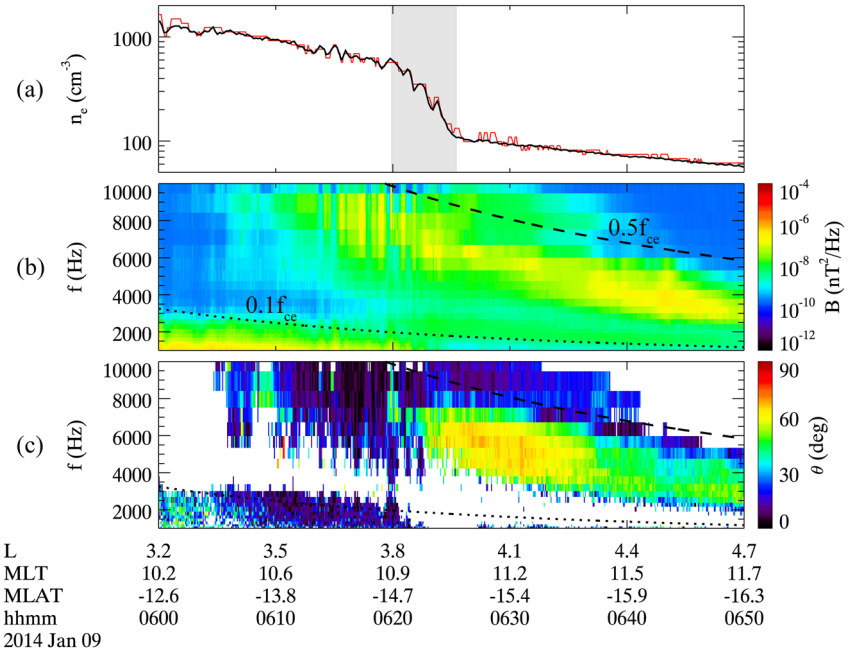

Figure 1. Measurements of the spacecraft passing through the plasmapause. (a) Electron density derived by spacecraft potential (black line), and upper hybrid band (red line). The spectrogram of (c) magnetic power B, and (c) wave normal angle θ. In both panels, the dotted and dashed lines represent 0.1 f_{ce} and 0.5 f_{ce} (f_{ce} is the local electron cyclotron frequency), respectively.

thickness (Figure 1b). Note that the observed whistler mode waves should be originally excited at the expected source region, that is, the magnetic equator (Kennel & Petschek, 1966), and then propagate to the higher-latitude location of the spacecraft. Using both the measured E and B of the waves it is found that the waves are propagating in a southward direction (not shown), consistent with the concept that they are coming from their equatorial source. What is interesting about the whistler mode wave propagation analyses is that near the inner edge of plasmapause (plasmasphere side), the waves have very small WNAs (≤20°). Waves around the outer edge (plasmatrough side) tend to have quite large WNAs (≥~60°).

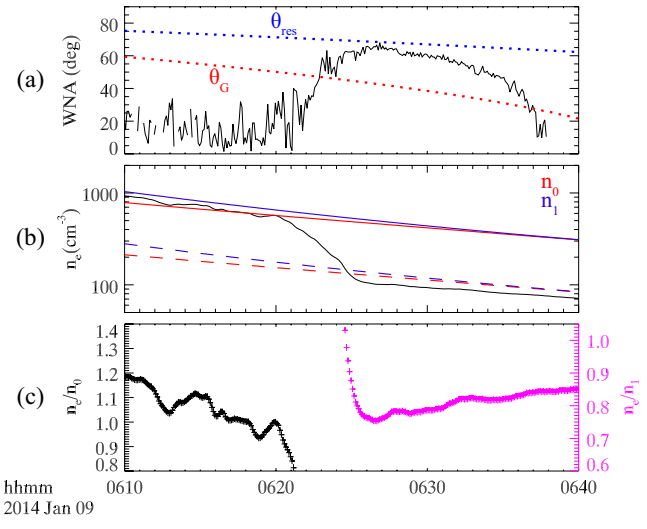

Figure 2. The analysis result based on ducting theory. (a) WNAs corresponding to the fixed wave frequency (f = 6320 Hz). The red and blue dotted lines represent the Gendrin angle θ_G and resonance angle θ_{res}, respectively. (b) Electron density with two critical densities n_0 (red) and n_1 (blue). (c) Relative density n_e/n_0 (black symbols), and n_e/n_1 (pink symbols).

To explain the different properties of the whistler mode waves around the two edges, we arbitrarily choose a typical wave with frequency f = 6.32 kHz for detailed modeling analyses. Figure 2a exhibits the WNA of this whistler mode only when its power is larger than 10^{-9} nT^2/Hz. The red and blue dotted lines indicate the Gendrin angle θ_G (i.e., arccos2f/f_{ce}, Gendrin, 1961) and resonance angle θ_{res} (i.e., arccosf/f_{ce}), respectively. From wave normal analyses, whistler mode waves near the inner edge (06:10–06:22 UT) are quasiparallel with small WNAs, while the waves are propagating quite obliquely to the ambient magnetic field (between θ_G and θ_{res}) around the outer edge of the plasmapause (06:23–06:37 UT). Following the theoretical model developed by Woodroffe and Streltsov (2013), two critical densities are calculated to identify the guiding effect of the plasmapause density gradient. The two critical densities are: $n_0 = \frac{m_e k_{\|}^2}{\mu_0 e^2}\left(\frac{f_{ce}}{f} - 1\right)$ and $n_1 = \frac{m_e k_{\|}^2}{\mu_0 e^2}\left(\frac{f_{ce}}{2f}\right)^2$. Here, m_e, e, μ_0 are the electron mass, electron charge, and vacuum permeability, respectively. The $k_{\|}$ is the parallel wave number, which is estimated by the dispersion relation of whistler mode waves in a cold plasma (Stix, 1962). For whistler mode waves on the inner edge of the plasmapause, the parallel wave

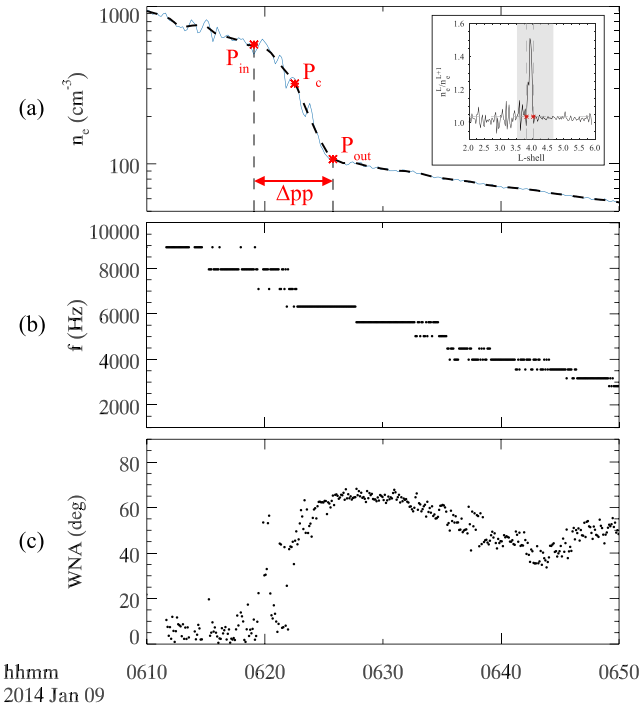

Figure 3. (a) Electron density (black dashed lines is the averaged density). P_{in}, P_{out}, and P_c represent the inner edge, outer edge, and center of the plasmapause, respectively. (b) Wave frequency corresponding to the peak magnetic power between 0.2 f_{ce} and 0.5 f_{ce}. (c) WNAs corresponding to the wave frequency in panel (b). The inserted panel in (a) presents the ratio of averaged density n_e^L to n_e^{L+1}. Here, n_e^{L+1} means one data point after n_e^L. Two red stars indicate the inner limit and outer limit of plasmapause.

number $k_{\|inner}$ is ~0.0031 rad/m, while $k_{\|outer}$ is ~0.0016 rad/m on the outer edge.

Figure 2b shows the measured densities during the interval, as well as the two critical densities. Solid lines are calculated based on $k_{\|inner}$, and dashed lines are calculated based on $k_{\|outer}$. According to the ducting theory (Streltsov & Bengtson, 2020; Streltsov et al., 2006; Woodroffe & Streltsov, 2013), if the electron density n_e satisfies $n_0 < n_e < n_1$, then the density gradient can be treated as a HDD-like density gradient. This is identified near the inner edge during ~06:10–06:20 UT. The HDD-like profile is also observed in Figure 2c (black symbols), which shows the ratio between n_e and n_0. Therefore, theoretically whistler mode waves with small WNAs will be confined within the region where the density ratio is larger than ~1.0, consistent with the region where quasi-parallel waves are detected (06:10–06:22; Figure 1a). Near the outer edge, the electron density satisfies $n_e < n_1$ (Figure 2b, blue dashed line), which is the criteria or a LDD-like density gradient. The profile of n_e/n_1 shown in Figure 2c (pink symbols) indicates that it is a LDD (~06:25–06:40). Combined with Figure 2a, we find that oblique waves with WNA between the Gendrin and resonant angles are well confined within the LDD-like density gradient. We have also analyzed whistler mode waves with other frequencies. In these cases, the results are quite similar (but are not shown for brevity). It is worth noting that the guiding effect of the plasmapause gradients results from both inhomogeneous magnetic fields and plasma densities (Woodroffe & Streltsov, 2013) rather than the typical density duct that is caused solely by the density variations (Streltsov & Bengtson, 2020; Streltsov et al., 2006). The plasma densities obtained from the spacecraft potential and upper hybrid band show very good consistency, suggesting the reliability of plasma density estimates. Even though there may exist the 10% uncertainty in the plasma density (Kurth et al., 2015; Wygant et al., 2013), according to the profile shown in Figure 2c, the 10% uncertainty will not change the trend and the principal conclusion remains unchanged.

4. Statistical Analysis

Taking this event as an example, we present the data processing in detail for the statistical study. At first, we average the electron density over 0.03 L (i.e., about ~60s, or ~6 data points), and get the profile of electron density versus L-shell. The panel inserted in Figure 3a presents the ratio of the averaged density n_e^L to n_e^{L+1}. Here, n_e^{L+1} indicates the next data point after n_e^L. The horizontal dashed line represents the mean value of ratio n_e^L / n_e^{L+1} in the entire region. The inner edge P_{in} and outer edge P_{out} are indicated by two red stars, which are defined by the sudden change of density gradient. Figure 3a (black dashed line) shows the averaged electron density between L = ~3.5 and L = ~4.7 (i.e., shaded region in the inserted panel). The positions of plasmapause center (P_c), its inner edge (P_{in}), and its outer edge (P_{out}) are indicated by red stars. P_c is defined as (Pin + P_{out})/2. Here we only record the L values of P_{in}, P_{out}, and P_c, since the density gradient is negligible in other two dimensions (MLT and MLAT). The width (Δpp) of the plasmapause is then given by P_{out}−P_{in}.

At each point in time (~6s interval), we record the frequency and WNA of whistler mode wave with the peak power from 0.2f_{ce} to 0.5f_{ce}. First, if the peak power is lower than 10^{-8} nT^2/Hz, then this time point will be discarded. Second, we only select the events away from the source region (i.e., magnetic equator) with |MLAT| > 5° in order to exclude the local generation effect. Figures 3b and 3c illustrate the results for this event. Whistler mode waves with WNAs smaller than ~20° are well confined near the inner edge, while those with large WNAs (>~50°) stay around the outer edge. Inside the plasmapause, there exists a trend

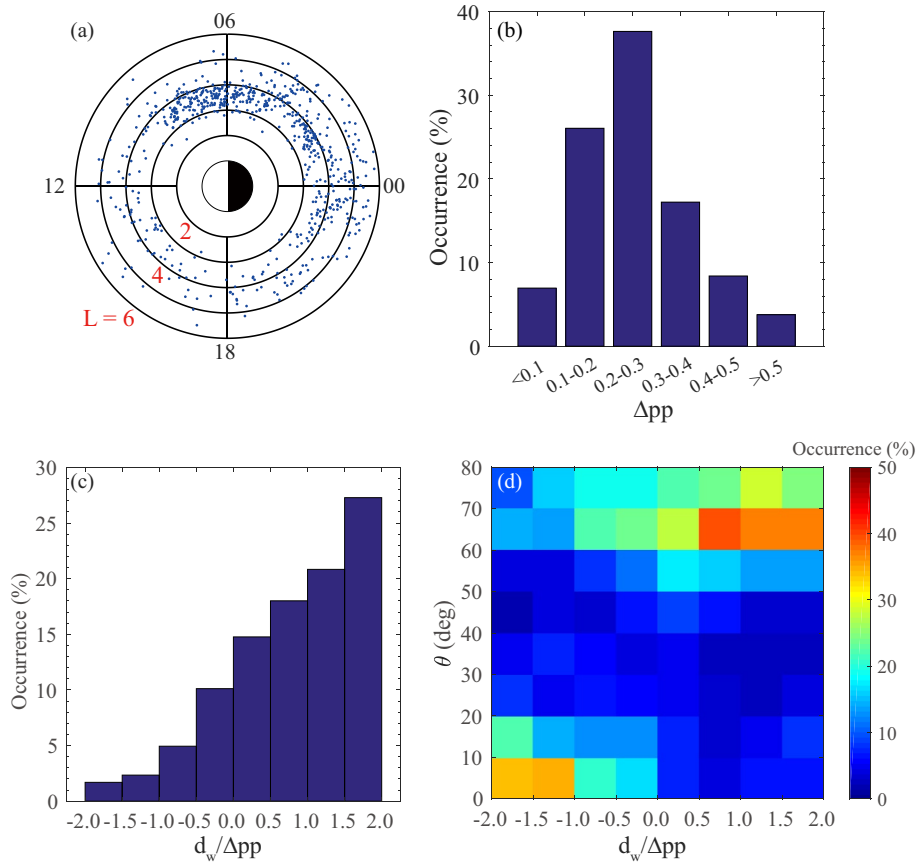

Figure 4. The distribution of (a) plasmapause center P_c in L-MLT plane, (b) plasmapause width Δpp, (c) normalized distance d_w/Δpp from the center of plasmapause for all recorded whistler mode waves, and (d) occurrence rate of whistler mode waves in the θ–d_w/Δpp plane. d_w/Δpp represents the distance between whistler mode wave and P_c normalized by Δpp. The positive d_w means the wave locates near the outer edge (plasmatrough side), while the negative d_w suggests the wave locates near the inner edge (plasmasphere side).

that the WNA of whistler mode waves increases as the electron density decreases. In addition, we also get the L value at each point in time, and calculate the distance (d_w) from the plasmapause center (P_c). Positive d_w values means the waves locate near the outer edge (plasmatrough side), while the negative d_w values indicates the waves are located near the inner edge (plasmasphere side).

We have analyzed 2-year (2013–2014) of data from both probes (RBSP A and B), and the results are shown in Figure 4, including the distributions of (a) plasmapause center P_c in the L-MLT plane, (b) plasmapause width Δpp, (c) normalized distance $d_w/\Delta pp$ from the center of plasmapause for all recorded whistler mode waves, and (d) occurrence rate of whistler mode waves in the θ–$d_w/\Delta pp$ plane. In our data base, there are 691 plasmapause crossings and ~36,000 wave recordings in total. In general, the plasmapause crossing occur mainly between $L = 3$ and $L = 4$ (Figure 4a). This is consistent with the statistical results of Carpenter and Anderson (1992). The selected events also have a higher occurrence in the morning sector, consistent with the local time of whistler mode chorus generation (Tsurutani & Smith, 1977; Merdith et al., 2003). In Figure 4b, we find that the plasmapause is quite dynamic and its width can vary from ~0.1 to ~0.5R_E. Therefore, we use the normalized distance d_w/Δpp to represent the position of each wave record relative to P_c for the purpose of removing the impact of various plasmapause widths. The recorded whistler mode waves are distributed in the d_w/Δpp range of −2.0 to +2.0, which are mainly detected near the outer edge of plasmapause (Figure 4c). Although the occurrence rate of whistler mode waves is less than 2% in the region of $-2.0<d_w/\Delta pp<-1.5$, there are still over 500 wave recordings to ensure reliability of this statistical study.

The WNAs of whistler mode waves show an expected but interesting distribution over the plasmapause. In Figure 4d (off-equator region), near the outer edge of plasmapause ($0.5<d_w/\Delta pp<2.0$), the overwhelming majority of whistler mode waves has very large WNAs, that is, larger than 50°, which suggest the outer edge can confine those oblique lower-band whistler mode waves just as the LDD does. Most whistler mode waves observed near the inner edge ($-2.0<d_w/\Delta pp<-0.5$) have very small WNAs, that is, smaller than 20°. This result is consistent with a guiding effect by the HDD. Near the plasmapause center, there is just a mixture of quasi-parallel and oblique whistler mode waves.

5. Summary and Discussion

In this paper, we present the observational support for the guiding effect of whistler mode waves by the plasmapause density gradients. Due to the combined effects of inhomogeneous magnetic field and plasma densities, whistler mode waves near the inner edge of plasmapause (plasmasphere side) will be guided by a HDD-like density gradient, and tend to have very small WNAs (≤20°). In contrast, whistler mode waves around the outer edge (plasmatrough side) guided by a LDD-like density gradient, tend to have quite large WNAs (≥∼60°). Moreover, our statistical analysis of whistler mode waves near the plasmapause indicates that the different wave properties found in one detailed case study is a general feature of waves present at the plasmapause.

Previous theoretical and simulation works have predicted that chorus waves can be ducted by the inner and outer edges of the plasmapause, but with different patterns (Inan & Bell, 1977; Woodroffe & Streltsov, 2013). The ideal direct evidence of wave ducting requires the joint observation by two or more probes at distant latitudes along one field line, which is too difficult to satisfy with existing data. Here we have analyzed one case in detail, and apply ducting theory (Streltsov & Bengtson, 2020; Streltsov et al., 2006; Woodroffe et al., 2013) to explain the distinct properties of whistler mode waves near inner and outer edges of plasmapause.

Observations and theoretical calculations (Artemyev, Agapitov, Breuillard, et al., 2012; Li, Mourenas, Artemyev, Agapitov, et al., 2014; Mourenas, Artemyev, Ripoll, et al., 2012; Ni et al., 2008) have shown that inclusion of oblique chorus waves could lead to a significant increase in pitch angle scattering rates than scattering by only quasi-parallel waves in the electron energy range of ∼200 eV to ∼2 MeV. Therefore, the two edges of the plasmapause may have different influences on energetic electron dynamics in the radiation belts. Thus this study may provide some new insights into energetic electron dynamics near the plasmapause.

Because it is possible that the observed different properties of whistler mode waves near the plasmapause may be associated with generation of the waves (Kennel & Petschek, 1966; LeDocq et al., 1998; Nunn et al., 1997; Omura et al., 2008; Tsurutani & Smith, 1974, 1977), we analyzed only whistler mode wave events away from the magnetic equator ($|MLAT| > 5°$). Thus we suggest that whistler mode wave guiding effects (Streltsov & Bengtson, 2020; Streltsov et al., 2006; Woodroffe & Streltsov, 2013) due to both the inhomogeneous magnetic field and plasma density are a reasonable explanation for the different wave properties near the plasmapause edge.

In the plasmatrough, oblique whistler mode waves are unstable in a plasma with low beta <0.025 (Fan et al., 2019; Gary et al., 2011; Yue et al., 2016;) or to beam-like electron distribution (Artemyev, Agapitov, Mourenas, et al., 2016; Li, Mourenas, Artemyev, Bortnik, et al., 2016; Mourenas, Artemyev, Agapitov, et al., 2015). Inside the plasmasphere, the high-frequency hiss waves with small WNAs can be generated by 1–2 keV injected electrons (He, Chen, et al., 2019; He, Yan, et al., 2020; He, Yu, et al., 2020). To verify that the observed wave features found in this study are not due to generation effects, the electron pitch angle distributions need to be studied. This will be performed in the near future. Since exohiss is considered as plasmaspheric hiss leakage at high latitudes, so the guiding effect of plasmapause may also contribute to the formation of exohiss as well (Bortnik et al., 2008; Zhu, Gu, et al., 2019; Zhu, Shprits, et al., 2018; Zhu, Su, et al., 2015).

Data Availability Statement

The data used in this study are available from the website: https://spdf.gsfc.nasa.gov/pub/data/rbsp/.

Acknowledgments
This research was funded by the Strategic Priority Research Program of Chinese Academy of Sciences Grant No. XDB41000000, the NSFC grant 41774151, 41631071, 41527804, Key Research Program of Frontier Sciences CAS(QYZDJ-SSW-DQC010), USTC Research Funds of the Double First-Class Initiative, the Fundamental Research Funds for the Central Universities, and Young Elite Scientists Sponsorship Program by CAST (2018QNRC001). The authors also acknowledge the entire Van Allen Probes instrument teams.

References

Artemyev, A., Agapitov, O., Breuillard, H., Krasnoselskikh, V., & Rolland, G. (2012). Electron pitch-angle diffusion in radiation belts: The effects of whistler wave oblique propagation. *Geophysical Research Letters*, *39*, L08105. https://doi.org/10.1029/2012GL051393

Artemyev, A., Agapitov, O., Mourenas, D., Krasnoselskikh, V., Shastun, V., & Mozer, F. (2016). Oblique whistler-mode waves in the Earth's inner magnetosphere: Energy distribution, origins, and role in radiation belt dynamics. *Space Science Reviews*, *200*, 261–355. https://doi.org/10.1007/s11214-016-0252-5

Bortnik, J., Thorne, R. M., & Meredith, N. P. (2008). The unexpected origin of plasmaspheric hiss from discrete chorus emissions. *Nature*, *452*, 62–66. https://doi.org/10.1038/nature06741

Bryant, D. A., Krimigis, S. M., & Haerendel, G. (1985). Outline of the active magnetospheric particle tracer explorers (AMPTE) mission. *IEEE Transactions on Geoscience and Remote Sensing*, *23*, 177. https://doi.org/10.1109/TGRS.1985.289511

Burtis, W. J., & Helliwell, R. A. (1969). Banded chorus: A new type of VLF radiation observed in the magnetosphere by OGO 1 and OGO 3. *Journal of Geophysical Research*, *74*, 3002–3010. https://doi.org/10.1029/JA074i011p03002

Carpenter, D. L. (1968). Recent research on the magnetospheric plasmapause. *Radio Science*, *3*, 719–725. https://doi.org/10.1002/rds196837719

Carpenter, D. L., & Anderson, R. R. (1992). An ISEE/whistler model of equatorial electron density in the magnetosphere. *Journal of Geophysical Research*, *97*, 489. https://doi.org/10.1029/91JA01548

Cornilleau-Wehrlin, N., Chauveau, P., Louis, S., Meyer, A., Nappa, J. M., Perraut, S., et al. (1997). The cluster spatio-temporal analysis of field fluctuations (staff) experiment. *Space Science Reviews*, *79*, 107–136. https://doi.org/10.1023/A:1004979209565

Fan, K., Gao, X., Lu, Q., Guo, J., & Wang, S. (2019). The effects of thermal electrons on whistler mode waves excited by anisotropic hot electrons: Linear theory and 2-D PIC simulations. *Journal of Geophysical Research: Space Physics*, *124*, 5234–5245. https://doi.org/10.1029/2019JA026463

Gao, X., Li, W., Thorne, R. M., Bortnik, J., Angelopoulos, V., Lu, Q., et al. (2014). New evidence for generation mechanisms of discrete and hiss-like whistler mode waves. *Geophysical Research Letters*, *41*, 4805–4811. https://doi.org/10.1002/2014GL060707

Gao, X., Lu, Q., & Wang, S. (2018). Statistical results of multiband chorus by using THEMIS waveform data. *Journal of Geophysical Research: Space Physics*, *123*, 5506–5515. https://doi.org/10.1029/2018JA025393

Gary, S. P., Liu, K., & Winske, D. (2011). Whistler anisotropy instability at low electron: Particle-in-cell simulations. *Physics of Plasmas*, *18*, 082902. https://doi.org/10.1063/1.3610378

Gendrin, R. (1961). Le guidage des whistlers par le champ magnetique. *Planetary and Space Science*, *5*, 274–282. https://doi.org/10.1016/0032-0633(61)90096-4

He, Z., Chen, L., Liu, X., Zhu, H., Liu, S., Gao, Z., & Cao, Y. (2019). Local generation of high-frequency plasmaspheric hiss observed by Van Allen Probes. *Geophysical Research Letters*, *46*, 1141–1148. https://doi.org/10.1029/2018GL081578

He, Z., Yan, Q., Zhang, X., Yu, J., Ma, Y., Cao, Y., & Cui, J. (2020). Precipitation loss of radiation belt electrons by two-band plasmaspheric hiss waves. *Journal of Geophysical Research: Space Physics*, *125*, e2020JA028157. https://doi.org/10.1029/2020JA028157

He, Z., Yu, J., Chen, L., Xia, Z., Wang, W., Li, K., & Cui, J. (2020). Statistical study on locally generated high-frequency plasmaspheric hiss and its effect on supra thermal electrons: Van Allen Probes observation and quasi-linear simulation. *Journal of Geophysical Research: Space Physics*, *125*, e2020JA028526. https://doi.org/10.1029/2020JA028526

Horne, R. B., Thorne, R. M., Shprits, Y. Y., Meredith, N. P., Glauert, S. A., Smith, A. J., & Decreau, P. M. E. (2005). Wave acceleration of electrons in the Van Allen radiation belts. *Nature*, *437*, 227–230. https://doi.org/10.1038/nature03939

Inan, U. S., & Bell, T. F. (1977). The plasmapause as a VLF wave guide. *Journal of Geophysical Research*, *82*, 2819–2827. https://doi.org/10.1029/JA082i019p02819

Karpman, V. I., & Kaufman, R. N. (1982). Whistler wave propagation in density ducts. *Journal of Plasma Physics*, *27*, 225–238. https://doi.org/10.1017/S0022377800026556

Kennel, C. F., & Petschek, H. E. (1966). Limit on stable trapped particle fluxes. *Journal of Geophysical Research*, *71*, 1–28. https://doi.org/10.1029/JZ071i001p00001

Kletzing, C. A., Kurth, W. S., Acuna, M., MacDowall, R. J., Torbert, R. B., Averkamp, T., et al. (2013). The electric and magnetic field instrument suite and integrated science (EMFISIS) on RBSP. *Space Science Reviews*, *179*, 127–181. https://doi.org/10.1007/s11214-013-9993-6

Koons, H. C. (1989). Observations of large-amplitude, whistler mode wave ducts in the outer plasmasphere. *Journal of Geophysical Research*, *94*. 15393–15397. https://doi.org/10.1029/JA094iA11p15393

Kurth, W. S., De Pascuale, S., Faden, J. B., Kletzing, C. A., Hospodarsky, G. B., Thaller, S., & Wygant, J. R. (2015). Electron densities inferred from plasma wave spectra obtained by the Waves instrument on Van Allen Probes. *Journal of Geophysical Research: Space Physics*, *120*, 904–914. https://doi.org/10.1002/2014JA020857

LeDocq, M. J., Gurnett, D. A., & Hospodarsky, G. B. (1998). Chorus source locations from VLF Poynting flux measurements with the Polar spacecraft. *Geophysical Research Letters*, *25*, 4063–4066. https://doi.org/10.1029/1998GL900071

Li, W., Bortnik, J., Thorne, R. M., Nishimura, Y., Angelopoulos, V., & Chen, L. (2011). Modulation of whistler mode chorus waves: 2. Role of density variations. *Journal of Geophysical Research*, *116*, A06206. https://doi.org/10.1029/2010JA016313

Li, W., Mourenas, D., Artemyev, A. V., Agapitov, O. V., Bortnik, J., Albert, J. M., et al. (2014). Evidence of stronger pitch angle scattering loss caused by oblique whistler-mode waves as compared with quasi-parallel waves. *Geophysical Research Letters*, *41*, 6063–6070. https://doi.org/10.1002/2014GL061260

Li, W., Mourenas, D., Artemyev, A. V., Bortnik, J., Thorne, R. M., Kletzing, C. A., et al. (2016). Unraveling the excitation mechanisms of highly oblique lower band chorus waves. *Geophysical Research Letters*, *43*, 8867–8875. https://doi.org/10.1002/2016GL070386

Li, W., Thorne, R. M., Bortnik, J., Nishimura, Y., Angelopoulos, V., Chen, L., et al. (2010). Global distributions of suprathermal electrons observed on THEMIS and potential mechanisms for access into the plasmasphere. *Journal of Geophysical Research*, *115*, A00J10. https://doi.org/10.1029/2010JA015687

Mauk, B. H., Fox, N. J., Kanekal, S. G., Kessel, R. L., Sibeck, D. G., & Ukhorskiy, A. (2013). Science objectives and rationale for the radiation belt storm Probes mission. *Space Science Reviews*, *179*. https://doi.org/10.1007/s11214-012-9908-y

Meredith, N. P., Horne, R. B., Thorne, R. M. & Anderson, R. R. (2003). Favored regions for chorus-driven electron acceleration to relativistic energies in the Earth's outer radiation belt. *Geophysical Research Letters*, *30*(16), 1871. https://doi.org/10.1029/2003gl017698

Moullard, O., Masson, A., Laakso, H., Parrot, M., Décréau, P., Santolik, O., & Andre, M. (2002). Density modulated whistler mode emissions observed near the plasmapause. *Geophysical Research Letters*, *29*(20). https://doi.org/10.1029/2002GL015101

Mourenas, D., Artemyev, A., Agapitov, O., Krasnoselskikh, V., & Mozer, F. S. (2015). Very oblique whistler generation by low-energy electron streams. *Journal of Geophysical Research: Space Physics*, *120*, 3665–3683. https://doi.org/10.1002/2015JA021135

Mourenas, D., Artemyev, A. V., Ripoll, J.-F., Agapitov, O. V., & Krasnoselskikh, V. V. (2012). Timescales for electron quasi-linear diffusion by parallel and oblique lower-band chorus waves. *Journal of Geophysical Research*, *117*, A06234. https://doi.org/10.1029/2012JA017717

Ni, B., Thorne, R. M., Shprits, Y. Y., & Bortnik, J. (2008). Resonant scattering of plasma sheet electrons by whistler-mode chorus: Contribution to diffuse auroral precipitation. *Geophysical Research Letters*, *35*, L11106. https://doi.org/10.1029/2008GL034032

Nunn, D., Omura, Y., Matsumoto, H., Nagano, I., & Yagitani, S. (1997). The numerical simulation of VLF chorus and discrete emissions observed on the Geotail satellite using a Vlasov code. *Journal of Geophysical Research*, *102*. 27083–27097. https://doi.org/10.1029/97JA02518

Omura, Y., Katoh, Y., & Summers, D. (2008). Theory and simulation of the generation of whistler-mode chorus. *Journal of Geophysical Research*, *113*, A04223. https://doi.org/10.1029/2007JA012622

Scarabucci, R. R., & Smith, R. L. (1971). Study of magnetospheric field oriented irregularities-the mode theory of bell-shaped ducts. *Radio Science*, *6*, 65–86. https://doi.org/10.1029/RS006i001p00065

Smith, R. L., & Angerami, J. J. (1968). Magnetospheric properties deduced from OGO 1 observations of ducted and nonducted whistlers. *Journal of Geophysical Research*, *73*, 1–20. https://doi.org/10.1029/JA073i001p00001

Smith, R. L., Helliwell, R. A., & Yabroff, I. W. (1960). A theory of trapping of whistlers in field-aligned columns of enhanced ionization. *Journal of Geophysical Research*, *65*, 815–823. https://doi.org/10.1029/JZ065i003p00815

Stix, T. H. (1962). *The theory of plasma waves* (p. 283). New York, NY: McGraw-Hill.

Streltsov, A. V., & Bengtson, M. T. (2020). Observations and modeling of whistler mode waves in the magnetospheric density ducts. *Journal of Geophysical Research: Space Physics*, *125*, e2020JA028398. https://doi.org/10.1029/2020JA028398

Streltsov, A. V., Lampe, M., Manheimer, W., Ganguli, G., & Joyce, G. (2006). Whistler propagation in inhomogeneous plasma. *Journal of Geophysical Research*, *111*, A03216. https://doi.org/10.1029/2005JA011357

Thorne, R. M., Li, W., Ni, B., Ma, Q., Bortnik, J., Chen, L., & Kanekal, S. G. (2013). Rapid local acceleration of relativistic radiation-belt electrons by magnetospheric chorus. *Nature*, *504*, 411–414. https://doi.org/10.1038/nature12889

Thorne, R. M., Ni, B., Tao, X., Horne, R. B., & Meredith, N. P. (2010). Scattering by chorus waves as the dominant cause of diffuse auroral precipitation. *Nature*, *467*, 943–946. https://doi.org/10.1038/nature09467

Tsurutani, B. T., Lakhina, G. S., & Verkhoglyadova, O. P. (2013). Energetic electron (>10 keV) microburst precipitation, ~5–15 s X-ray pulsations, chorus, and wave-particle interactions: A review. *Journal of Geophysical Research: Space Physics*, *118*(5), 2296–2312. https://doi.org/10.1002/jgra.50264

Tsurutani, B. T., & Smith, E. J. (1974). Postmidnight chorus: A substorm phenomenon. *Journal of Geophysical Research*, *79*, 118–127. https://doi.org/10.1029/Ja079i001p00118

Tsurutani, B. T., & Smith, E. J. (1977). Two types of magnetospheric ELF chorus and their substorm dependences. *Journal of Geophysical Research*, *82*, 5112. https://doi.org/10.1029/JA082i032p05112

Woodroffe, J. R., & Streltsov, A. V. (2013). Whistler propagation in the plasmapause. *Journal of Geophysical Research*, *118*, 716–723. https://doi.org/10.1002/jgra.50135

Woodroffe, J. R., Streltsov, A. V., Vartanyan, A., & Milikh, G. M. (2013). Whistler propagation in ionospheric density ducts: Simulations and DEMETER observations. *Journal of Geophysical Research*, *118*, 7011–7018. https://doi.org/10.1002/2013JA019445

Wygant, J. R., Bonnell, J. W., Goetz, K., Ergun, R. E., Mozer, F. S., Bale, S. D., et al. (2013). The electric field and waves instruments on the radiation belt storm probes mission. *Space Science Reviews*, *179*, 183–220. https://doi.org/10.1007/s11214-013-0013-7

Yue, C., An, X., Bortnik, J., Ma, Q., Li, W., Thorne, R. M., et al. (2016). The relationship between the macroscopic state of electrons and the properties of chorus waves observed by the Van Allen probes. *Geophysical Research Letters*, *43*, 7804–7812. https://doi.org/10.1002/2016GL070084

Zhu, H., Gu, W., & Chen, L. (2019). Statistical analysis on plasmatrough exohiss waves from the Van Allen Probes. *Journal of Geophysical Research: Space Physics*, *124*, 4356–4364. https://doi.org/10.1029/2018JA026359

Zhu, H., Shprits, Y. Y., Chen, L., Liu, X., & Kellerman, A. C. (2018). An event on simultaneous amplification of exohiss and chorus waves associated with electron density enhancements. *Journal of Geophysical Research: Space Physics*, *123*, 8958–8968. https://doi.org/10.1029/2017JA025023

Zhu, H., Su, Z., Xiao, F., Zheng, H., Wang, Y., Shen, C., et al. (2015). Plasmatrough exohiss waves observed by Van Allen Probes: Evidence for leakage from plasmasphere and resonant scattering of radiation belt electrons. *Geophysical Research Letters*, *42*, 1012–1019. https://doi.org/10.1002/2014GL062964